Application of the LIDAR technology for obstacle detection during the operation of agricultural vehicles

Z. Doerr[1], A. Mohsenimanesh[2], C. Laguë[2*] and N.B. McLaughlin[3]

[1]*Buchan, Lawton, Parent Ltd., 18 Curity Avenue, Toronto, ON, M4B 1X7 Canada*
[2]*Department of Mechanical Engineering, University of Ottawa, Ottawa, ON, K1N 6N5 Canada*
[3]*Eastern Cereal and Oilseed Research Centre, Agriculture and Agri-Food Canada, Ottawa, ON, K1A 0C6 Canada*
**Email: Claude.Lague@uottawa.ca*
http://dx.doi.org/10.7451/CBE.2013.55.2.9

Doerr, Z., A. Mohsenimanesh, C. Laguë and N.B. McLaughlin. 2013. **Application of the LIDAR technology for obstacle detection during the operation of agricultural vehicles.** Canadian Biosystems Engineering/Le génie des biosystèmes au Canada **55**: 2.9-2.16. Many algorithms have been proposed in the literature for the detection of foreign objects or obstacles to the operation of autonomous vehicles. However, a comparative evaluation of these existing approaches is still lacking. In this study, multiple feature recognition algorithms (average height, density, connectivity, and discontinuity methods) were evaluated for the identification of three types of foreign objects placed in four types of crops (range of crop height: 20 – 80 cm) under different field and operating conditions. The field experiments were completed using a SICK laser measurement system (LMS) 291-S14 scanner that was placed on a tractor to scan standing crops in which the standard test objects had been placed. The data collected by the sensor was analyzed using the software MATLAB 2D and 3D versions. The average height method allowed for a 72.4% average object detection rate while the connectivity method only resulted in a successful object detection rate of 18% for all the experiments. It was also found that the crop density or foliage cover had a negative impact on the detection rate for shorter test objects with the higher rates of obstacle detection being achieved for objects significantly taller than crops. Increasing vehicle speed was also found to reduce detection abilities due to lower scan resolution per distance travelled. **Keywords:** Laser Measurement System, object detection, crops, foreign objects, autonomous vehicles, safety.

Plusieurs algorithmes ont été développés pour déterminer la position d'objets pouvant entraver le fonctionnement de véhicules autonomes. Il reste cependant à compléter une évaluation comparative de ces différentes approches. Dans le cadre de cette étude, l'efficacité de quatre algorithmes de reconnaissance et de détection d'obstacles (méthodes basées sur la hauteur moyenne, la densité, la connectivité et la discontinuité) pour la détection de trois types d'obstacles placés dans quatre types de récolte différentes (gamme de hauteur des plantes : 20 – 80 cm) a été comparée pour différentes combinaisons de conditions d'opération au champ. Les tests ont été complétés à l'aide d'un capteur SICK de mesure au laser (LMS) 291-S14 installé sur un tracteur agricole afin de détecter des objets placés à des endroits prédéterminés à proximité de la trajectoire du tracteur. Les données recueillies par le capteur ont été analysées à l'aide du logiciel MATLAB (versions 2D et 3D). La méthode de la hauteur moyenne a permis d'atteindre un taux de détection global des obstacles au champ de 72,4% alors que la méthode de la connectivité a fourni les résultats les moins intéressants avec un taux de détection global de seulement 18%. Les résultats obtenus indiquent également que la taille des cultures ainsi que la densité du couvert végétal ont résulté en des taux de détection des obstacles moins élevés. Les taux de détection ont également été moins élevés dans le cas des obstacles de petite taille alors que les taux de détection des objets dont la hauteur dépasse celle des cultures étaient plus élevés. L'accroissement de la vitesse d'avancement du tracteur a eu un impact négatif sur le taux de détection des obstacles. **Mots-clés:** système de détection laser, détection d'obstacles, cultures, véhicule autonome, sécurité.

INTRODUCTION

Autonomous agricultural vehicles bring a new concern to the safety of agricultural field operations. While autonomous agricultural vehicles can improve operator safety by removing human operators from the vehicles, they can also result in increased safety concerns related to the risks of collisions with humans, animals, or other vehicles in their vicinity. Therefore, it is essential to provide autonomous vehicles with obstacle detection and collision avoidance systems (Kise et al. 2005). Examples of such systems developed for other applications include multiple mobile robots in a 3-D environment collision avoidance function to coordinate the motion of all robots operating on the same site (Yamashita et al. 2003) and obstacle avoidance and path planning system for underwater vehicles based on a multi-beam forward looking sonar sensor (Petillot et al. 2001).

With advances in sensing technology, various types of sensors for distance measurement between static or mobile objects (Fresquet Periu 2012; Lee and Ehsani 2008 and 2009) and for position, attitude and direction-of movement information have been developed which can be used in autonomous agricultural vehicles (Keicher and Seufert 2000). These sensors include mechanical systems, global navigation satellite systems (GNSS), machine vision, laser triangulation, as well as ultrasonic and geomagnetic devices (Keicher and Seufert 2000). It is critically important that the sensors used on any machine be optimal in terms of the tasks performed by the vehicle, the environmental conditions in which it operates, and overall costs (Powell and Boyette 2005).

Effective and robust computational methods are essential to detect image features by image processing or to deal with sensor data fusion successfully for providing the

basic information required by agricultural vehicle autonomous guidance systems. Therefore, the choice and implementation of method and signal processing algorithms are very important (Li et al. 2009). Several algorithms have been used for detecting obstacles or for obstacle mapping. Kise et al. (2005) used a template matching function and a Kalman filter to detect the location of an obstacle. The Hough transform method has been applied for robust recognition of plant rows in the application of machine vision on agricultural vehicle guidance system (Åstrand and Baerveldt 2005; Marchant and Brivot 1995). Other researchers have used the Occupancy Grid Density algorithm to map the fault tolerant sensor for robotic vision (Meyer-Delius et al. 2012; Elfes 1989).

Autonomous off-road navigation is central to several important applications of unmanned ground vehicles especially for finding route, which can be used to detect, identify or modify routing on the expected paths (Matthies et al. 2005). Obstacle detection and avoidance issues must be addressed in the development of autonomous agricultural vehicles because of obvious safety concerns (Powell and Boyette 2005). Millimetre wave radars as well as SICK Light Detection And Ranging (SICK LIDARs) were used in off-highway obstacle detections systems for the Grand Challenge competition organized by the Defense Advanced Research Projects Agency (DARPA). Both systems were simultaneously used to profit from their respective advantages while minimizing their shortcomings (Johnston 2006). Millimetre wave radar with a Charge Coupled Devices (CCD) camera was used for obstacle detection (Sugimoto et al. 2004). Other scientists have detected obstacles, mapped and navigated using Laser Scanners LMS in agricultural applications (Lee and Ehsani 2008).

Measuring the surface topography of soil and plants or accurately determining the shape of an object is important for many precision agriculture applications. For this, laser scanners have shown great potential (Lee and Ehsani 2008). Extensive information has been published on the subject of safe operation of autonomous agricultural vehicles, including findings on systems developed and used to detect and identify obstacles on the expected paths followed by the vehicles. However, due to the stand density, height or leaf area of various crops, in-situ investigations are required to distinguish between potential obstacles to machine operation and the crops. Moreover, many algorithms that deal with the detection of foreign objects or obstacles have been proposed in the literature. However, a comparative evaluation of the existing approaches is still lacking.

The overarching goal of the research work reported herein was to assess the effectiveness of the LIDAR technology at detecting obstacles in agricultural fields. The end purpose was to detect fixed objects that may negatively impact the operation of autonomous agricultural machines. The specific objectives were: 1. to evaluate the effectiveness of different signal processing algorithms for a specific LMS LIDAR sensor, and 2. to identify the effects of different crop, field, and operation parameters on obstacle detection.

MATERIALS AND METHODS

The LIDAR used in this study was a LMS 291-S14 (Sick Ag, Germany) which is a non-contact measurement system in stand-alone operation for industrial applications. This equipment scans its surroundings two-dimensionally with a radial field of vision using infrared laser beams (laser radar). Measurement data are available in real-time and can be used for further processing or control tasks. This particular scanner was intended for an outdoor use, had a 90° scan angle, a 0.5° resolution, a 10 mm accuracy, and a

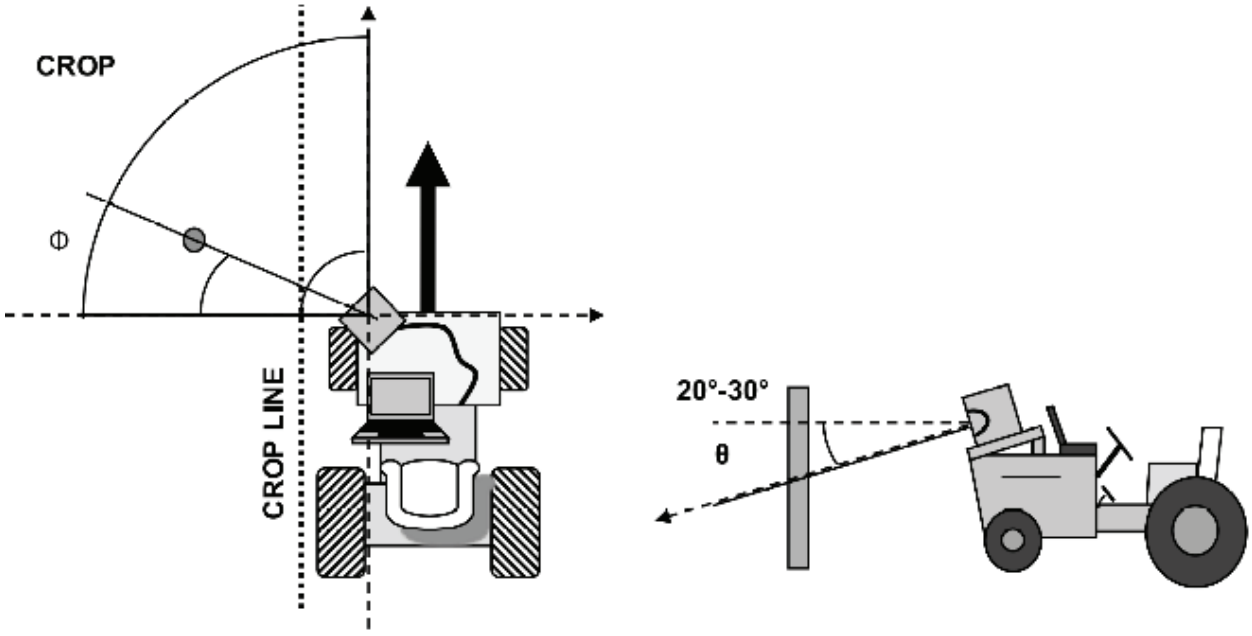

Fig. 1. Mounting of the Laser Scanner on the tractor.

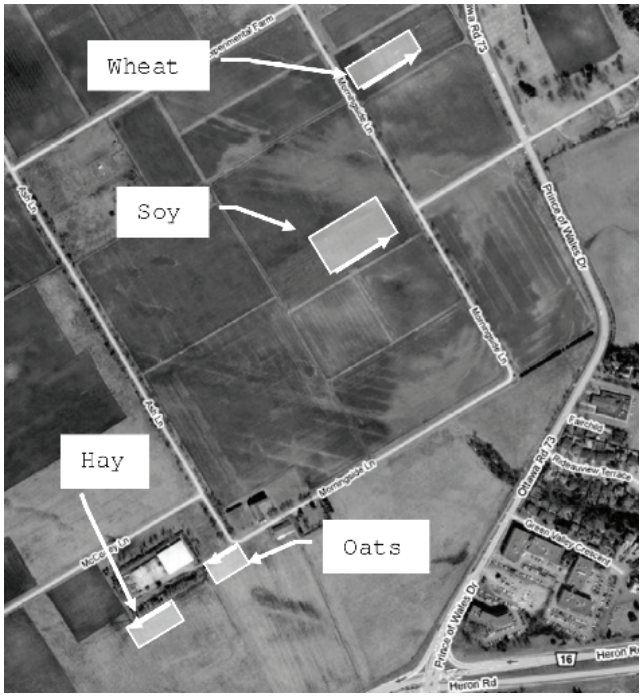

Fig. 2. Satellite view of experimental sites at the Central Experimental Farm, Ottawa, ON.

13.3 ms response time (75Hz) (Sick Sensor Intelligence 2006).

The LIDAR was installed at the front of a commercial agricultural tractor (Kubota B6200) above the crop line (Fig. 1). The scanning plane was oriented down from the horizontal at 20° and 30°. The 90° scan plane was oriented to the left of the path of the tractor to cover the second quadrant of the Cartesian plane with 90° being the direction of travel. The scanner was oriented in this direction to minimize the scanning of the vehicle tracks caused by repetitive passes as well as the reflectivity for each range set. For each complete scan, there were 181 values returned, ranging from 0° to 90° in 0.5° increments. The data received from the scanner are represented in polar coordinates with the scanner as the origin (r, θ and φ in Fig. 1).

The experimental site was located at the Eastern Cereal and Oilseed Research Centre of Agriculture and Agri-Food Canada in Ottawa, Ontario. Figure 2 shows the exact location for each test sites as well as arrows representing the tractor test path. The experiments were completed in four different crops: wheat, hay, soybeans, and oats. The average heights of these different crops were 20 to 40 (hay), 60 (oats), 70 (soybeans), and 75 cm (wheat) when the experiments were completed.

Three types of test object were used: tall square-shaped box (1.83 m height by 0.17 m width), tall cylindrical-shaped box (1.83 m height by 0.14 m diameter), short-cylindrical-shaped box (0.6 m height by 0.14 m diameter). The shorter test object was used to assess the ability of the system to scan and detect objects that were approximately the same height or shorter than the average crop canopy. The tall square, tall cylindrical,

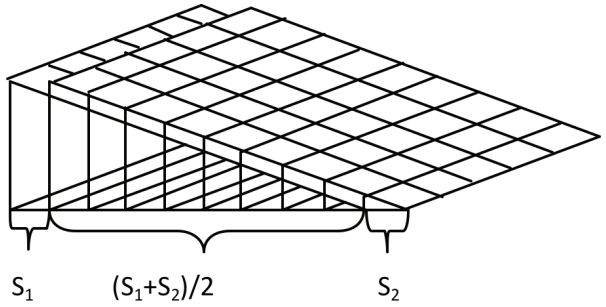

Fig. 3. Map matrices using a contour style.

and the short cylindrical objects were labelled TS, TC and SC respectively. The test objects were made from cardboard and wood, which have a reflectivity of 20% and 40% respectively (Sick Sensor Intelligence 2006). A reference flag was placed 10 m behind the objects along the crop edge and was used as a reference point for each field scan.

The field obstacle detection experiments were completed at three different operating speeds (2, 4, and 7 km/h) using two different scanning angles θ (20 and 30 degrees), and at various stages of growth of the different crops. A total of 292 field tests were completed.

Image processing

The software used to record the data was a Measurement Software Tool (MST) program provided by SICK. This program records the range data directly from the LMS sensor and converts the data into text files that are then inserted into data matrices using MATLAB software. Each value represents the distance recorded with the column number corresponding to the scan angle value increasing by 0.5° for each column and then these polar points were converted into Cartesian values. The experimental data collected during the field trials were analyzed using the average height, connectivity, density, and discontinuity methods (Doerr 2010).

Average Height Method

Using the 181 Cartesian points for each scan, an occupancy grid was created and the points were fitted into the grid. The size of each grid could change depending of the speed of the vehicle as well as the time between each scan. In the x-direction, the grid size was kept constant at 10 cm. In the y-direction the distance per scan was used. To calculate the distance per scan, the vehicle velocity V (m/s) was divided by the scan frequency f (Hz):

$$Dist_scan = V/f \quad (1)$$

Then, the predicted height for each point was calculated by knowing the height and orientation of the LMS. The measured height of the mounted scanner was 1.17 m, and θ being either 20 or 30 degrees depending on the type of test:

$$Z_{pts} = H - Y_{pts}(\sin\theta) \quad (2)$$

where, Z_{pts} is calculated height of range data point, Y_{pts} is the range data value from LMS, θ is scan angle, 20° or 30°, and H is measured height of the LMS.

An occupancy grid matrix with height values was obtained in grids where points were detected and a value of zero for all others. For each scan, an occupancy grid was created and then superimposed on an overall map matrix. Because each grid size was equal to the distance travelled between scans, each occupancy matrix was overlapped by one column. This means that a new column was then added to the map matrix with each additional scan. For all other columns, where there was an overlap with previous values, the new and old values were averaged for a new cell value, corresponding to an average calculated height. The final map matrices were then plotted using a contour style, which highlights higher cell values (Fig. 3).

$$Map = S_1 + (S_1 + S_2)/2 + S_2 \quad (3)$$

Equation 3 is used to create and increase the size of the map. S_1 represents the sections of the map where there was no new information to be added; $(S_1+S_2)/2$ is the middle section where new information is being added to the map. The final S_2 section represents a completely new section of the map where no known information was available. The process is repeated for every new scan with the S1 section growing by one row with every scan. It should be noted that the cell values for each method are calculated prior to the data fusion. The middle section for the connectivity and density method is slightly different because the sum of the values are used and not the average. The middle section is then represented by (S_1+S_2). The final map matrices are then plotted using a contour style, which highlights higher cell values.

Occupancy grid density method

This method was very similar to the average height method where the Cartesian points were sorted into their appropriate grid values. The primary difference for this method was that the cell value for each occupancy cell corresponds to the number of data points found in each cell. Each cell value represents the density of data points found within that specific grid area. The map matrix was created using a slightly different method as the average height method. In this method the density values were summed and not averaged.

Occupancy grid density and connectivity method

Building on the density method, another algorithm was added, called connectivity. When multiple grid squares were found to be attached, either by side or diagonal, their connectivity factor was increased. This method multiplies the density values found in the previous section by each cells connectivity value. This increases the value of each cell by a factor that corresponds to its group size.

Crop Discontinuity (Hough Transform)

To form contour lines based on the data points, a generalized contour of the crops was created. When a height discontinuity was found and the difference in Y values for two adjacent contour lines were greater than the specified threshold, the location was noted and plotted on the map matrix of the overall pass. Data points from the occupancy grid were used to create contour lines within 3-grid-wide strips, approximately 30 cm. One contour line was created within each 3- column-wide-strip outputting 2 data points representing the start and finish points of the line. The Y-values of each adjacent point were compared and put into a discontinuity matrix if the differences in values were greater than a specified threshold.

The programs used for the implementation of the four algorithms are freely available for research purposes upon request to the corresponding author.

RESULTS and DISCUSSION

The experimental data collected during the field trials were analyzed using the average height, connectivity, density, and discontinuity methods. The results obtained from these different analyses were then compared using the following parameters: cell values at each object location, average cell values and standard deviations in the area surrounding the objects, and the presence of false detections or excessive noise. For all four methods, the results were considered successful when peaks in cell values were found near the known object locations and noted unsuccessful when no peak in cell value was found at the known locations of the objects. For the discontinuity method, the mean distance of the discontinuities to the known object location and visual inspection of clustering were used to distinguish successful tests. The test was also marked as successful when the mean distance of discontinuities diminished with an increase in threshold and clustering of discontinuities around the flag or objects were found.

Average Height Method

The average height method consistently yielded the best results for cell value in the four different crops that were used during the experiments. This method yielded very high cell values at the grid location of the objects with an average cell value of 1014 and a standard deviation of 201. This method also found very little noise with cell values around the object to be in the order of 1.0, or three orders of magnitude lower. A typical example of the composed map view of a test run is presented in Fig. 4.

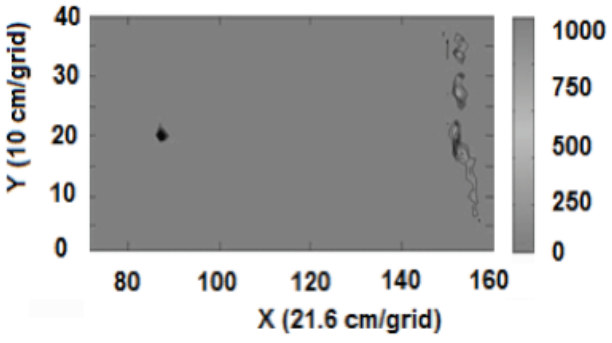

Fig. 4. Obstacle detection results using the average height method (hay crop, tall square object, 20 degrees scan angle, speed of 7 km/h).

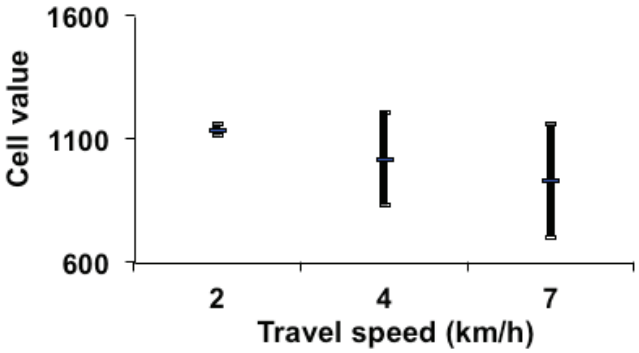

Fig. 5. Average height method results at different speeds.

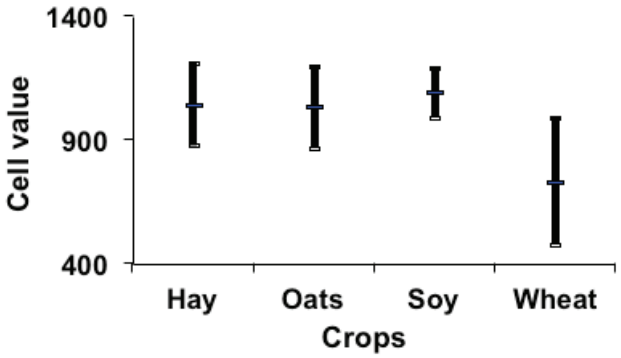

Fig. 6. Average height method results for different crops.

The tractor travelled along the x-axis below the matrix and the object was placed near cell (87, 20) as indicated in the figure. Cell values for the entire scanned area were very low with the exception of the last section (i.e. x > 15.0 m) for which the scan values were not averaged out. This phenomenon was present in most results obtained by this method. Though the cell values do not represent the actual height of objects or of the crop, the average height method does yield the desired large differences between the location of objects of higher heights and the rest of the field. Although this method has the best overall results, it was not capable of detecting the shorter objects.

The average cell values and their standard deviations are represented at the location of the object obtained under different travel speed conditions (Fig. 5). The average cell values decreased with increasing travel speed from 1142 at 2 km/h to 934 at 7 km/h. This was caused by the decrease of field resolution with an increase in vehicle speed. Because of the decreased number of datum points having higher average height cell values, the cell values at the object location have less of an opportunity to be averaged higher than their surroundings. It should also be noted that the standard deviation of height results increased with increasing travel speed, from 24 at 2 km/h to 228 at 7 km/h.

Figure 6 shows the average cell values and their standard deviations at the location of the object obtained with different crops (hay, oats, and soybeans) with the average height method. The cell values at the object location varied depending on the type of crop present in the experimental plots. For soybeans and oats, the average cell values as well as the standard deviations were very similar with a difference of only 59 between the average cell values. The wheat average detection values were slightly lower at 730 and had a greater standard deviation at 257.

The differences in the results obtained for the two scanner angles used during the field experiments were very small. The results obtained from the 20-degree tests yielded a higher average cell value (+3.4%) and a lower standard deviation (-8.9%) at the object location than those from the 30-degree tests. This shows that the 20° scan angle provided a slightly greater distinction between the objects and the surrounding fields. The effects of objects type and height were investigated and the analysis of the experimental data did not allow for the identification of the short 60-cm objects that were placed in the experimental plots (Fig. 7). All of the cell values for the short cylindrical object, at the known object location, were between 0 and 1.0, which were the same values as the rest of the field. In summary, there was no increase in cell values for the short cylindrical object. The average cell value for the two tall objects having square and cylindrical cross sections were very similar with slightly higher and smaller standard deviation for the cylindrical one. At different stages of growth for the soybean and hay crops, the only significant change in values was the standard deviation, which doubled in value for the end-of-season tests. This may be caused by the loss of leaves near the end of the season, which allowed for greater range penetration into the foliage. In the early-season tests, the soybean canopy was dense and did not allow for much line of sight penetration.

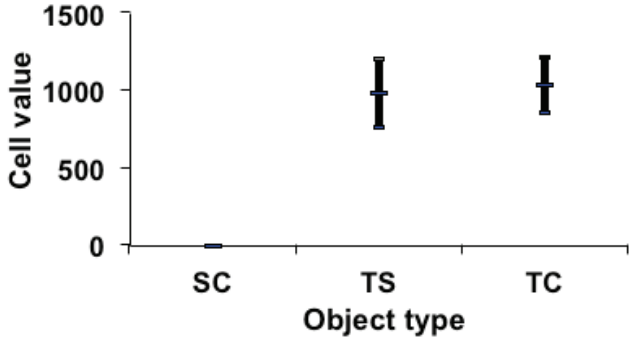

Fig. 7. Average height method results for different types of objects.

Density method

Object detection rate, which was the percentage of correct image cells entities in the detected set, were similar to those obtained with the average height method, but with slightly higher noise as seen in Fig. 8. The noise values were found to be generally below the object values, suggesting the ability to establish a threshold value that could eliminate much of the false detections. With the data analysis methods described above, there were very few successful object detections for the shorter test object.

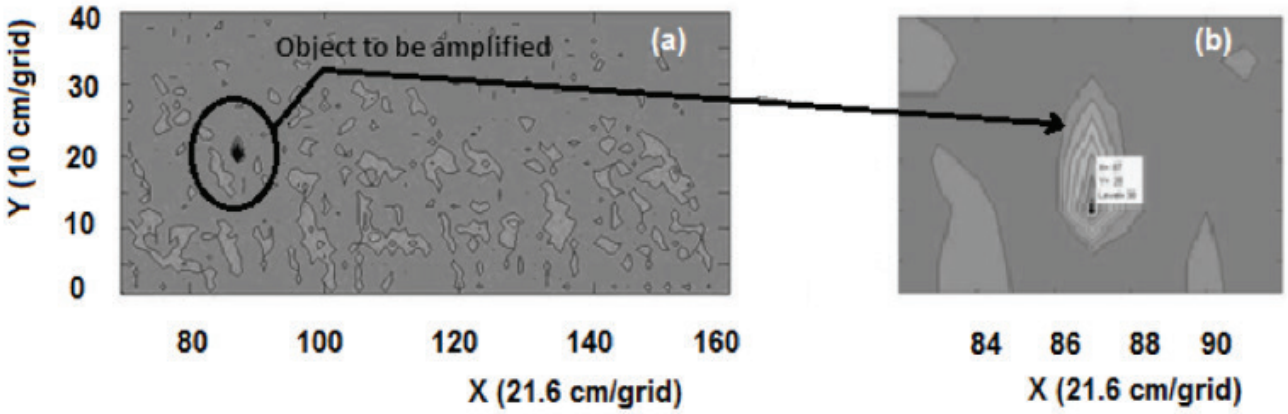

Fig. 8. Example of results obtained using the density method: (a) object with slightly higher noise, and (b) the amplified object.

Only six unconfirmed peaks were measured in the oat and hay crops; three in each the oat and hay crops with five of the tests run at 4 km/h and the other at 7 km/h.

The density method shows to be more effective at detecting the objects at slower speeds (Fig. 9). As expected, because of the higher crop resolution, the grid density at the locations of the test objects is higher at slower speeds. The average cell values are 47, 38 and 31 range data points at 2, 4 and 7 km/h respectively at the grid location of the test objects.

The cell values for each crop type are shown in Fig. 10. The hay crop cell values vary the most with a standard deviation of 22 points but with the highest average cell value at 48. The hay crop provided the highest cell value because of the shorter crop height at 0.20 m and 0.40 m. The LMS has a longer view of the objects during each field test thus providing a greater number of data points at the object location. The wheat field provide the lowest amount of cell value at the object locations with an average cell value of 26. Because of the greater density and greater wheat crop height, 0.75 m, the LMS has less of a view of the objects during each field run. The overall object location cell value for all tests has an average of 37 and a standard deviation of 19.

The hay crop provided the clearest values showing a clear peak in density at the object locations on the map matrix. Unfortunately very little success with the shorter 60-cm object was found. Less than 10% of the short object tests provided any distinguishable change in the density around the object location.

The analysis showed that there was very little overall difference when comparing the cell values for the two scan-angles of 20 and 30 degrees. The cell values for the tall cylindrical object were significantly higher than for the tall square and short cylindrical objects (Fig. 11). The effects of objects type showed that there was no success rate on the square and cylindrical objects. Effects of growth stage of the soybeans crops were investigated and the results showed that the cell values increased slightly from 29 to 32 from early to late season. It is believed that the crop canopy has an effect on these values similar to the average height method. With a decrease in crop canopy, the LMS may have greater view of the objects below the average crop height which could increase the number of data points at or near the object locations.

Connectivity method

The detection rates of the objects were very low for the connectivity method. The primary reason for this low success rate is the increased noise caused by the connectivity algorithm itself. The connectivity algorithm connects much of occupancy grids that were created by the crop foliage. Because the connected foliage or crop components are greater than the connected object grids, greater values were placed around the objects. The

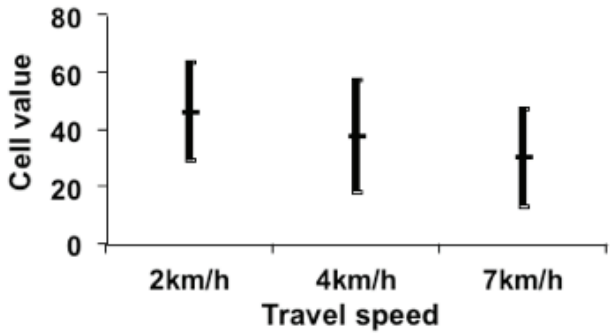

Fig. 9. Density method results for different speeds.

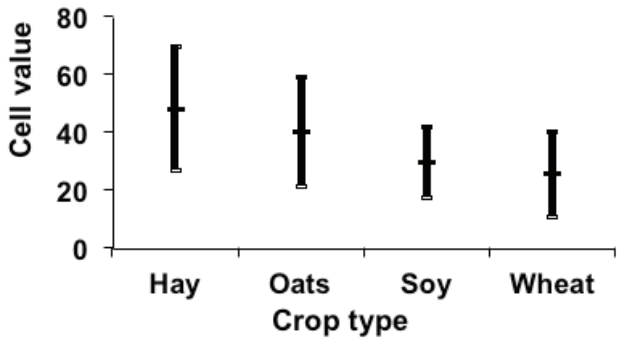

Fig. 10. Density method results for different crops.

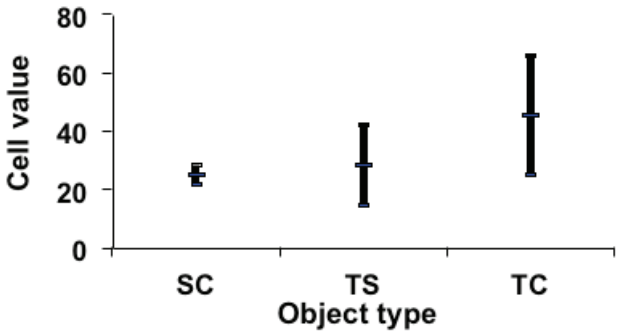

Fig. 11. Density method results for different types of objects.

expected connection values caused by the objects were less than or similar to those caused by the crop canopy. It was expected to have a diffusion of range data points through the crop and a large clustering and high connection and/or clustering at the test objects.

The average cell values of the map were also compared to the cell values of the test object locations. The peak values were all above the average cell values in all of the results. For the potential peaks only 1 of 28 tests had a peak value lower than the field average. In the tests where no peaks were detected, approximately half of the object location values were greater than the field average. Detailed analyses relative to the effects of speed, scanner angle, type of crops, type of objects, and growth stage of the crops have not been completed because of the general ineffectiveness of this method of data analysis in detecting the objects placed in the experimental plots.

Discontinuity method

In order to analyze the ability of the Hough Transform to detect crop and object edges, the edge variance threshold was varied with the threshold value representing the allowable distance between two adjacent Hough Transform points. The average distances of each discontinuity point to the object location for a varying threshold were compared. The MATLAB function used to determine the distance between two points uses the map grid locations and not actual distances. Thus, the mean distance and standard deviation did not accurately represent in-field distance values. Due to the increased computational and time requirements of the discontinuity tests, this method was not used for all the recorded tests. At least one of each type of test was used for this method for a total of 63 different test types. Each one of those scan results were tested at various thresholds. The threshold was increased until clustering occurred or only a few discontinuities remained.

Overall assessment

Each proposed detection method yielded a different overall object detection rate. The greatest success was achieved with the average height method, which resulted in an overall 72.4% object detection rate. The lowest detection rate method was the connectivity, which could only provide higher peak values for 18% of the tests (Fig. 12).

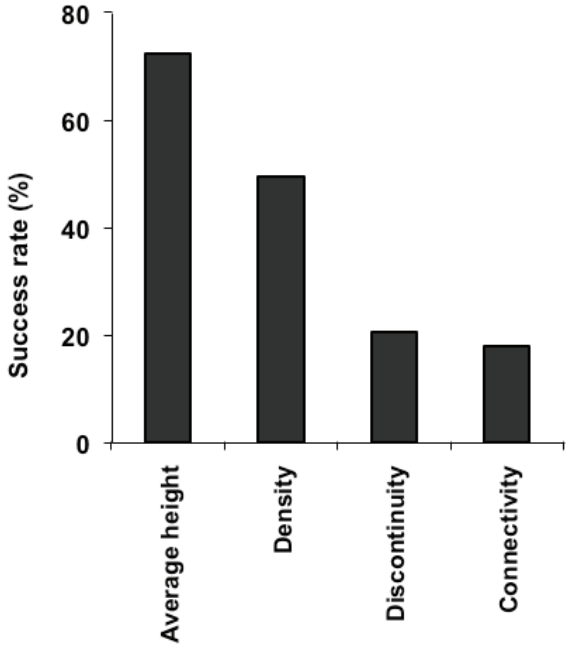

Fig. 12. Overall obstacle detection rates for the four signal processing algorithms.

From a safety perspective, only a detection level of 100% would be satisfactory and none of the algorithms evaluated were able to meet that criterion.

CONCLUSION

1. The connectivity method yielded the lowest detection rate with only 18% of the results showing peak values at the known object location. The discontinuity method, when analysing the relative mean and standard deviation of the discontinuities to the known object location, yielded converging results for 20.6% of the tests. The density and average height method were shown to have the greatest success rates of 49.4% and 72.4% respectively. The density method had the greatest noise. There was very little success in detecting the shorter test object.
2. Both the average height and density method cell values decreased with an increase in vehicle operating speed. The discontinuity method had greater success at higher speeds. A total of 26.9% of high-speed tests yielded good results whereas only 8.33% for the slower travel speed.
3. The average height method yielded the best results with the hay, oats, and soybeans crops with the wheat crop providing the lowest cell values. Using the density method the highest cell values were obtained from the hay crops and the lowest from the wheat. The discontinuity method experienced consistently low average distance results with the wheat crop.

For all methods the tall cylindrical object yielded slightly higher values than the tall square object.

ACKNOWLEDGEMENT

The authors thank the Natural Sciences and Engineering Research Council of Canada for financial support of this research, and Dr. Pierre Payeur, Associate Professor, School of Electrical Engineering and Computer Science, Faculty of Engineering, University of Ottawa for his valuable input on many of the object detection algorithms that were used in this study.

REFERENCES

Åstrand, B. and A.J. Baerveldt. 2005. A vision based row-following system for agricultural field machinery. *Mechatronics* 15(2): 251-269. http://dx.doi.org/10.1016/ j.mechatronics.2004.05.005

Doerr, Z. 2010. Evaluating the ability to detect foreign objects in crops using laser range scanners mounted on agricultural vehicles. Unpublished M.Sc. thesis. Ottawa, ON: Department of Mechanical Engineering, University of Ottawa.

Fresquet Periu, C. 2012. Isolating vibrations on laser range scanners mounted on agricultural vehicles to improve the detection of foreign objects. Unpublished M.Sc. thesis. Ottawa, ON: Department of Mechanical Engineering, University of Ottawa.

Johnston, J. 2006. Off-highway obstacle detection. *IEEE Instrumentation & Measurement Magazine* 9(5): 16-24. http://dx.doi.org/10.1109/MIM.2006.1708345

Elfes, A. 1989. Using occupancy grids for mobile robot perception and navigation. *IEEE Computer* 22 (6): 46 – 57. http://dx.doi.org/10.1109/2.30720

Keicher, R. and H. Seufert. 2000. Automatic guidance for agricultural vehicles in Europe. *Computers and Electronics in Agriculture* 25: 169-194. http://dx.doi.org/10.1016/S0168-1699(99)00062-9

Kise, M., Q. Zhang, and N. Noguchi. 2005. An obstacle identification algorithm for a laser range finder-based obstacle detector. *Transactions of the ASAE* 48(3): 1269-1278. http://dx.doi.org/10.13031/2013.18491

Lee, K.H. and R. Ehsani. 2009. A laser scanner based measurement system for quantification of citrus tree geometric characteristics. *Applied Engineering in Agriculture* 25 (5): 777-788. http://dx.doi.org/10.13031/2013.28846

Lee, K.H. and R. Ehsani. 2008. Comparison of two 2D laser scanners for sensing object distances, shapes, and surface patterns. *Computers and Electronics in Agriculture* 60(2): 250-262. http://dx.doi.org/10.1016/ j.compag.2007.08.007

Li, M., K. Imou, K. Wakabayashi and S. Yokoyama. 2009. Review of research on agricultural vehicle autonomous guidance. *International Journal of Agriculture and Biology Engineering* 2(3): 1-16.

Marchant, J and R Brivot. 1995. Real-time tracking of plant rows using a Hough Transform. *Real-Time Imaging* 1: 363-371. http://dx.doi.org/10.1006/rtim.1995.1036

Matthies, L., C. Bergh, A. Castano, J. Macedo, and R. Manduchi. 2005. Obstacle detection in foliage with ladar and radar. *Robotics Research* 15: 291-300.

Meyer-Delius, D., M. Beinhofer and W. Burgard. 2012. Occupancy grid models for robot mapping in changing environments. In *Proceedings Twenty-Sixth AAAI Conference on Artificial Intelligence*, 2024-2030. Toronto, Canada. July 22-26.

Petillot, Y., I.T. Ruiz, and D.M. Lane. 2001. Underwater vehicle obstacle avoidance and path planning using a multi-beam forward looking sonar. *IEEE Journal of Oceanic Engineering* 26(2): 240-251. http://dx.doi.org/10.1109/48.922790

Powell, N.B. and M.D. Boyette. 2005. A sensor integration method for autonomous equipment. ASABE Paper No: 051137, ASAE Annual Meeting. St. Joseph, MI: ASAE.

Sick Sensor Intelligence. 2006. LMS200/211/221/291 Laser Measurement Systems: Technical Description.http://sicktoolbox.sourceforge.net/docs/sick-lms-technical-description.pdf (2013/10/11).

Sugimoto, S. and H. Tateda, H. Takahashi, and M. Okutomi. 2004. Obstacle detection using millimeter-wave radar and its visualization on image sequence. In *Proceedings17th IEEE International Conference on Pattern Recognition*, 342-345 (vol. 3). Cambridge, UK. August 23-26.

Yamashita, A., T. Arai, J. Ota, and H. Asama. 2003. Motion planning of multiple mobile robots for cooperative manipulation and transportation. *IEEE Transactions on Robotics and Automation* 19(2): 223-237. http://dx.doi.org/10.1109/TRA.2003.809592